Available online at www.sciencedirect.com
SCIENCE DIRECT®
Journal of Sound and Vibration 283 (2005) 915–926
JOURNAL OF SOUND AND VIBRATION
www.elsevier.com/locate/jsvi

On the volume oscillations of a tethered bubble

A.O. Maksimov*

Pacific Oceanological Institute and also Instiitute of Marine Technology Problem, Far Eastern Branch of the Russian Academy of Sciences, 43 Baltic Street, Vladivostok 690041, Russia

Received 5 January 2004; received in revised form 18 May 2004; accepted 19 May 2004

Abstract

The behaviour of a gas bubble tethered to a rigid plane boundary in an oscillatory pressure field is investigated by means of image theory. The inversion method is utilised to obtain an exact solution. This method is based on invariance of the Laplace equation to conformal transformations. The modified Rayleigh equation for the volume pulsation has been derived. It follows directly from this equation that the fundamental — the so-called 'Minnaert' frequency — for the tethered bubble depends on the contact angle and this dependence is not monotonic.
© 2004 Elsevier Ltd. All rights reserved.

When a gas bubble in a liquid is insonified, it may undergo volume pulsation. The acoustic output of such an oscillating bubble has been recorded in the sound of many phenomena. There are a number of acoustical techniques for bubble sizing. The effectiveness of these techniques is investigated in laboratory studies for simple controlled populations (stationary single tethered bubble) [1,2]. However, the influence of the boundary: wire [1], glass rode [2], or glass plate [3] on the bubble dynamics in an oscillating pressure field remains unclear.

On the other hand, many attempts have been made by numerous researchers to study the interaction between a bubble and a rigid boundary [4–7]. The boundary integral method is a suitable way to simulate the problem of interaction of a bubble with a boundary and provides good agreement between the numerical prediction and the experimental data.

*Tel.: +7 4232 313081; fax: +7 4232 312573.
E-mail address: maksimov@poi.dvo.ru (A.O. Maksimov).

0022-460X/$ - see front matter © 2004 Elsevier Ltd. All rights reserved.
doi:10.1016/j.jsv.2004.05.021

In this study we present an analytical approach using image theory concerning the behaviour of a gas bubble near a rigid plane boundary, that gives a better physical insight into the dynamics of tethered bubbles.

Consider an air bubble of radius R_0 driven by an acoustical wave of amplitude P_m and angular frequency ω. As the radius of the bubble is often much smaller than the acoustic wavelength λ (i.e. $R/\lambda = R\omega/c_0 \ll 1$, where c_0 is the sound speed in the liquid), there is effectively an 'inner' region around the bubble which may be regarded as incompressible. These ideas were exploited by Prosperetti [8] and others in derivation of the weakly compressible spherical-bubble equation. The extension this approach to nonspherical bubbles has been given by Blake et al. [7]. We neglect viscous forces because the boundary layers are typically very thin around the bubble surface, so in any event viscous forces are confined to the immediate proximity of the surface of the bubble. Thus the bubble dynamics may be modelled by considering the fluid to be inviscid and irrotational, leading to the velocity being expressed as the gradient of a potential φ, i.e.

$$\mathbf{v} = \nabla\varphi, \quad \nabla^2\varphi = 0. \tag{1}$$

The geometry of the problem is illustrated in Fig. 1. The basic bubble equilibrium shapes show a segment of spherical profile, and the contact angle ϑ_c is the angle obtained when this shape is

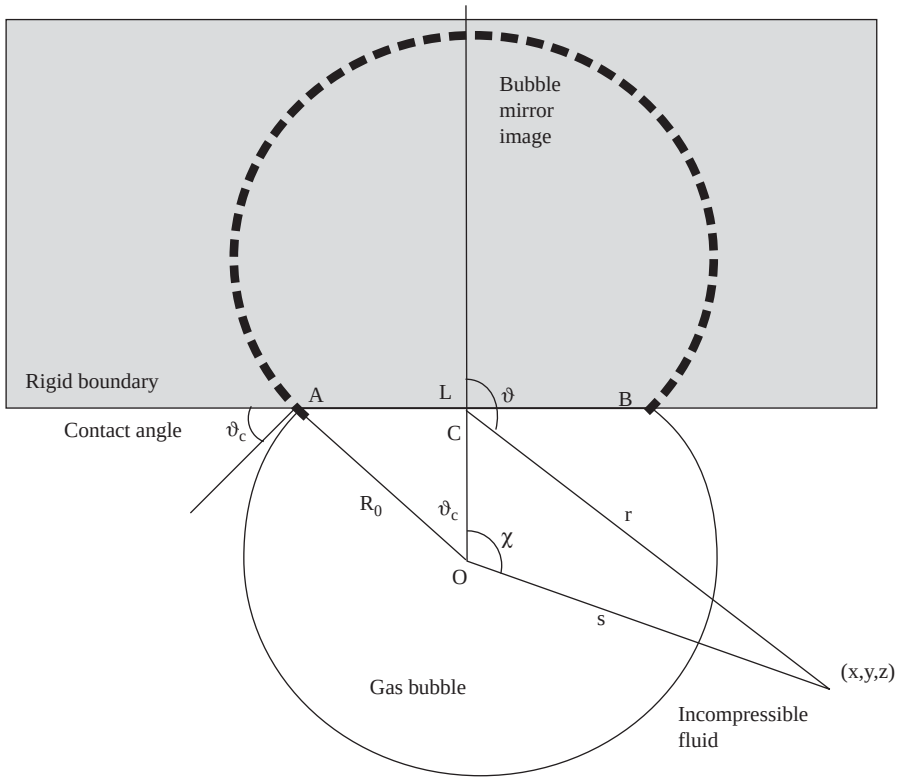

Fig. 1. The basic bubble equilibrium shapes show a segment of spherical profile, and the contact angle ϑ_c is the angle obtained when this shape is extrapolated to the solid surface. The diameter of the ring of contact is denoted by L. The presence of the rigid boundary can be replaced by the mirror image of the bubble relative to the plane $z = 0$.

extrapolated to the solid surface. The magnitude of ϑ_c depends on wetting by the liquid of the material of the boundary and on the surface tension of the bubble wall. The diameter of the ring of contact is denoted by L. The relation between L and the equilibrium radius of the bubble R_0 is given by $L = 2R_0 \sin \vartheta_c$ and the volume of the spherical segment is

$$V_0 = \frac{4\pi}{3} R_0^3 \left[1 - \frac{(1 - \cos \vartheta_c)^2 (2 + \cos \vartheta_c)}{4}\right].$$

The condition of no flow across the rigid boundary requires

$$\frac{\partial \varphi}{\partial z} = 0 \text{ on } z = 0. \tag{2}$$

The pressure in the liquid P is governed by the Bernoulli equation

$$P(\mathbf{r}, t) + \rho_0 \left[\dot{\varphi}(\mathbf{r}, t) + (\nabla \varphi)^2/2\right] = P_\infty + P_m \sin(\omega_p t) + \rho_0 \dot{\varphi}_\infty(t), \tag{3}$$

where ρ_0 and P_∞ are the equilibrium density and pressure, and P_m is the amplitude of the driving wave. As the potential in the Bernoulli equation is defined within an arbitrary function of time, the potential at large distances from the bubble wall $\varphi_\infty(t)$ is commonly taken to be zero, but we choose another normalisation of this variable.

The dynamic boundary condition is that the pressures on the two sides of the bubble wall differ only because of surface tension, i.e. if P_l and P_g denote the pressure in the water and in the bubble respectively, then

$$P_l = P_g - \frac{\sigma}{\rho_0}(\nabla \cdot \mathbf{n}), \quad P_g = P_0 (V_0/V)^\gamma, \tag{4}$$

where $\mathbf{n}$ is the unit vector normal to the bubble surface, σ is the coefficient of surface tension. We adopt a polytropic law for the gas in the bubble and V, V_0 are the instantaneous and equilibrium bubble volume, γ is the polytropic exponent, P_0 is the equilibrium pressure in the bubble.

The kinematic boundary condition takes the form [9]

$$\left[\frac{\partial}{\partial t} + (\mathbf{v} \cdot \nabla)\right](s - R)_{s=R_0+v} = 0, \quad s = \sqrt{x^2 + y^2 + (z + R_0 \cos \vartheta_c)^2}. \tag{5}$$

The use of the image method to model the flow around a bubble near a rigid boundary has been first proposed by Cole [10], but we shall follow the approach derived by Kobelev and Ostrovskii [11]. As the pressure within the bubble is practically constant when $R/\lambda \ll 1$ (homobaric bubble), its surface is equipotential if one neglects surface tension and the nonlinear inertial term in Bernoulli equation (3). We shall analyse only linear volume oscillations of relatively large bubbles $R_0 \gg 1\ \mu$m, therefore can use this analogy with electrostatics. The velocity field $\mathbf{v}$ in the liquid near the bubble wall will correspond to the electric field strength $\mathbf{E}$ near the conducting body of the same shape. The normal component of the velocity on the bubble wall will be an analog of the surface charge density. The total charge Q will correspond to

$$Q \sim \oint_S v_n \, \mathrm{d}S = \frac{\mathrm{d}V}{\mathrm{d}t}.$$

The presence of the rigid boundary can be replaced by the mirror image of the bubble relative to the plane $z = 0$ (see Fig. 1) and thus the boundary conditions (2) will by automatically satisfied.

We derive an exact solution by use the inversion method [11,12]. This method is based on invariance of the Laplace equation to the definite class of transformation. Really the Laplace equation in spherical coordinates has the form

$$\frac{1}{r^2}\frac{\partial}{\partial r}\left(r^2\frac{\partial\varphi}{\partial r}\right)+\frac{1}{r^2}\nabla_\Omega^2\varphi=0,$$

where ∇_Ω^2 is an angular part of Laplacian. It is easy to verify that this equation conserve its form under transformation

$$r'=\frac{l^2}{r}\ \text{(inversion)}, \tag{6a}$$

if one transforms unknown function φ according to

$$\varphi=\frac{r'}{l}\varphi', \tag{6b}$$

here l is the radius of inversion. Thus if $\varphi(\mathbf{r})$ is a solution of Laplace equation, than

$$\varphi'(\mathbf{r}')=\frac{l}{r'}\varphi\left(\frac{l^2}{r'^2}\mathbf{r}'\right) \tag{7}$$

is also a solution.

Put the origin of the spherical system of coordinate in the point A (see Fig. 1) and transform our problem with inversion radius equal to $l = L = 2R_0 \sin\vartheta_c$. The point B will be

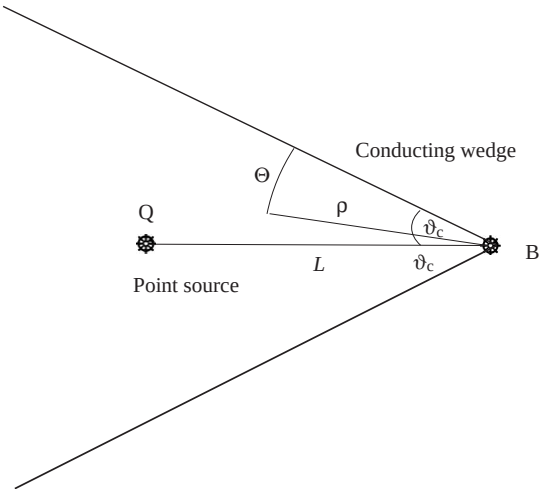

Fig. 2. The inversion of the bubble tethered to the rigid wall problem. The bubble wall and the bubble wall mirror are transferred into a wedge with an angle equal to $2\vartheta_c$. Point at infinity will go to the origin of coordinates, the point B on the contact curve is unchanged and the point A goes to point at infinity.

unchanged, the point A will go to point at infinity, and point at infinity will go to the origin of coordinates $r' = (L^2/r)$, the bubble wall and the bubble wall mirror will transfer into a wedge with an angle equal to $2\vartheta_c$ (see Fig. 2). Choosing the normalisation of φ such a way that its equipotential value vanishes on the bubble wall will lead to nonzero value of potential 'at infinity' φ_∞. For the inverted potential it leads to the point source at the origin that redistribute charge density on the 'conducting' planes of the wedge where $\varphi' = 0$. The solution of this problem: point charge in conducting wedge is good known [13,14].

The potential $\varphi'(r')$ is given by the formulae

$$\varphi' = \frac{Q}{2\vartheta_c\sqrt{2L\rho}}\int_\eta^\infty \left[\frac{\sinh\left(\frac{\pi\xi}{2\vartheta_c}\right)}{\cosh\left(\frac{\pi\xi}{2\vartheta_c}\right) - \cos\left(\frac{\pi(\theta-\vartheta_c)}{2\vartheta_c}\right)} - \frac{\sinh\left(\frac{\pi\xi}{2\vartheta_c}\right)}{\cosh\left(\frac{\pi\xi}{2\vartheta_c}\right) - \cos\left(\frac{\pi(\theta+\vartheta_c)}{2\vartheta_c}\right)}\right] \times \frac{\mathrm{d}\xi}{\sqrt{\cosh\xi - \cosh\eta}}. \tag{8}$$

Here the cylindrical system of coordinates is used with the axis z' along the line of corner points, the angle θ is counted off wedge plane (see Fig. 2), $\cosh\eta = (L^2 + \rho^2 + z'^2)/(2L\rho)$.

The auxiliary solution (8) provide the solution of our problem. Performing inverse transformation (6a,b), (7) we obtain for Cartesian coordinate system with the origin at point C:

$$\varphi(x,y,z,t) = \frac{Q(t)}{2\sqrt{2}\vartheta_c\left[\left(x^2+y^2+z^2-L^2/4\right)^2 + z^2L^2\right]^{1/4}} \times \int_{\eta(x,y,z)}^\infty \left[\frac{\sinh\left(\frac{\pi\xi}{2\vartheta_c}\right)}{\cosh\left(\frac{\pi\xi}{2\vartheta_c}\right) - \cos\left\{\frac{\pi[\theta(x,y,z)-\vartheta_c]}{2\vartheta_c}\right\}} - \frac{\sinh\left(\frac{\pi\xi}{2\vartheta_c}\right)}{\cosh\left(\frac{\pi\xi}{2\vartheta_c}\right) - \cos\left\{\frac{\pi[\theta(x,y,z)+\vartheta_c]}{2\vartheta_c}\right\}}\right] \times \frac{\mathrm{d}\xi}{\sqrt{\cosh\xi - \cosh\eta(x,y,z)}}, \tag{9}$$

where

$$\cosh\eta(x,y,z) = \frac{x^2+y^2+z^2+(L^2/4)}{\sqrt{\left[x^2+y^2+z^2-(L^2/4)\right]^2 + z^2L^2}},$$

and

$$\theta(x,y,z)=\vartheta_c+\arccos\left\{\frac{x^2+y^2+z^2-(L^2/4)}{\sqrt{\left[x^2+y^2+z^2-(L^2/4)\right]^2+z^2L^2}}\right\}.$$

It is easy verify that at the bubble wall: $x^2+y^2+(z+R_0\cos\vartheta_c)^2=R_0^2$ the phase $\theta=2\vartheta_c$ and potential (9) vanishes.

Far from the bubble $[x^2+y^2+z^2]^{1/2}\gg L$ the potential is approached to

$$\varphi(x,y,z,t)\xrightarrow[[x^2+y^2+z^2]\to\infty]{}\frac{Q(t)}{L}=\frac{Q(t)}{2R_0\sin\vartheta_c},$$

thus $\dot{\varphi}_\infty$ contained in Bernoulli integral (3) is equal to

$$\dot{\varphi}_\infty=\frac{\dot{Q}(t)}{2R_0\sin\vartheta_c}. \tag{10}$$

To find the displacement bubble wall we should substitute solution (9) into the kinematic boundary condition (5). The normal derivation at the bubble wall has the simplest form in the spherical coordinate system with the origin coincided with the centre of the bubble, when

$$\frac{\partial\varphi}{\partial n}=\left.\frac{\partial\varphi}{\partial s}\right|_{s=R_0}=\dot{v}(\kappa),\ s=\sqrt{x^2+y^2+(z+R_0\cos\vartheta_c)^2},\ \cos(\kappa)=(z+R_0\cos\vartheta_c)/s.$$

By use the fact that $\varphi\big|_{s=R_0}=0$, we obtain

$$\dot{v}(\kappa)=\left.\frac{\partial\varphi}{\partial s}\right|_{s=R_0}=\frac{Q(t)}{R_0^2}\frac{\pi}{4\sqrt{2}\vartheta_c^2}\frac{\sin\vartheta_c}{(\cos\vartheta_c-\cos\kappa)^{3/2}}\times\int_{\cosh^{-1}\left(\frac{1-\cos\vartheta_c\cos\kappa}{\cos\vartheta_c-\cos\kappa}\right)}^{\infty}\frac{\mathrm{d}\xi}{\sqrt{\cosh\xi-\dfrac{1-\cos\vartheta_c\cos\kappa}{\cos\vartheta_c-\cos\kappa}}}\frac{\sinh\left(\dfrac{\pi\xi}{2\vartheta_c}\right)}{\cosh^2\left(\dfrac{\pi\xi}{2\vartheta_c}\right)}. \tag{11}$$

This expression defines the way the normal displacement of bubble wall v depends on azimutal angle κ.

The volume of the bubble V and its time derivation are easily expressed through the normal displacement

$$V=\int_{\vartheta_c}^{\pi}\int_0^{2\pi}\frac{(R_0+v(\kappa))^3}{3}\sin\kappa\,\mathrm{d}\kappa\,\mathrm{d}\alpha\simeq V_0+2\pi R_0^2\int_{\vartheta_c}^{\pi}v(\kappa)\sin\kappa\,\mathrm{d}\kappa, \tag{12a}$$

$$\frac{\mathrm{d}V}{\mathrm{d}t}=2\pi R_0^2\int_{\vartheta_c}^{\pi}\dot{v}(\kappa)\sin\kappa\,\mathrm{d}\kappa. \tag{12b}$$

Substituting the expression for normal displacement (11) into Eq. (12b) we obtain desirable result

$$\frac{\mathrm{d}V}{\mathrm{d}t} = CQ, \quad \dot{\varphi}_\infty = \frac{1}{2R_0 \sin\vartheta_c C(\vartheta_c)} \frac{\mathrm{d}^2 V}{\mathrm{d}t^2},$$
$$C(\vartheta_c) = \frac{\pi^2}{2\sqrt{2}\vartheta_c^2} \int_{\vartheta_c}^{\pi} \frac{\sin\vartheta_c \sin\kappa \, \mathrm{d}\kappa}{(\cos\vartheta_c - \cos\kappa)^{3/2}}$$
$$\times \int_{\cosh^{-1}\left(\frac{1-\cos\vartheta_c\cos\kappa}{\cos\vartheta_c-\cos\kappa}\right)}^{\infty} \frac{\mathrm{d}\xi}{\sqrt{\cosh\xi - \dfrac{1-\cos\vartheta_c\cos\kappa}{\cos\vartheta_c-\cos\kappa}}} \frac{\sinh\left(\dfrac{\pi\xi}{2\vartheta_c}\right)}{\cosh^2\left(\dfrac{\pi\xi}{2\vartheta_c}\right)}. \tag{13}$$

Evaluating Bernoulli integral at bubble wall we get an analog of Rayleigh equation for the volume pulsation of tethered bubble

$$P_\infty + P_m \sin(\omega_p t) + \rho_0 \dot{\varphi}_\infty(t) = P(s = R_0, t) = P_0 \left(V_0/V\right)^\gamma \approx P_0(1 - \gamma \Delta V/V_0),$$
$$\frac{1}{2R_0 \sin\vartheta_c C(\vartheta_c)} \frac{\mathrm{d}^2 V}{\mathrm{d}t^2} + \frac{\gamma P_0}{\rho_0 V_0} \Delta V = -\frac{P_m}{\rho_0} \sin(\omega t). \tag{14}$$

It follows directly from this equation that the fundamental frequency of the tethered bubble has the form

$$\Omega_0^2(R_0, \vartheta_c) = \frac{2\gamma R_0 \sin\vartheta_c C(\vartheta_c) P_0}{\rho_0 V_0} = \Omega_0^{*2}(R_0) \frac{\sin\vartheta_c C(\vartheta_c)}{2\pi\left[1 - \dfrac{(1-\cos\vartheta_c)^2(2+\cos\vartheta_c)}{4}\right]}, \tag{15}$$

where $\Omega_0^*(R_0) = \sqrt{3\gamma P_0/\rho_0} R_0^{-1}$ is the fundamental frequency of a free bubble.

The integral form of the derived expressions (9), (11), (13) makes it rather immense, therefore we present solutions for a set of particular values of contact angle when integrals can be calculated in a closed form:

- $$\vartheta_c = \pi/2, \quad L = 2R_0, \quad \varphi = \frac{Q}{2}\left[\frac{1}{(x^2+y^2+z^2)^{1/2}} - \frac{1}{R_0}\right], \quad \dot{v} = -\frac{Q}{2R_0^2}, \quad C = \pi,$$
$$\Omega_0^2\left(R_0, \frac{\pi}{2}\right) = \Omega_0^{2*}(R_0), \tag{16}$$

- $$\vartheta_c = \pi/4, \quad L = \sqrt{2}R_0,$$
$$\varphi = Q\left[\frac{1}{\sqrt{2}R_0} + \frac{1}{2(x^2+y^2+z^2)^{1/2}}\right.$$

$$-\frac{1}{\sqrt{2}\sqrt{x^2+y^2+(z-R_0/\sqrt{2})^2}}-\frac{1}{\sqrt{2}\sqrt{x^2+y^2+(z+R_0/\sqrt{2})^2}}\Bigg],$$

$$\dot{v}=\left.\frac{\partial\varphi}{\partial s}\right|_{s=R_0}=\frac{Q}{\sqrt{2}R_0^2}\left\{1-\left[3-2\sqrt{2}\cos\kappa\right]^{-3/2}\right\},\quad C=\sqrt{2}\pi\left[1+2^{-1/2}\left(3+2\sqrt{2}\right)^{-1/2}\right],$$

$$\Omega_0^2\left(R_0,\frac{\pi}{4}\right)=\Omega_0^{2*}(R_0)\frac{\left[1+2^{-1/2}\left(3+2\sqrt{2}\right)^{-1/2}\right]}{2\left[1-\left(2-5\sqrt{2}/4\right)/4\right]}\approx 0.686\Omega_0^{2*}(R_0). \tag{17}$$

For the symmetric case

- $$\vartheta_c=3\pi/4,\quad L=\sqrt{2}R_0,$$

$$\varphi=Q\left[\frac{1}{\sqrt{2}R_0}-\frac{1}{2(x^2+y^2+z^2)^{1/2}}\right.$$

$$\left.-\frac{1}{\sqrt{2}\sqrt{x^2+y^2+(z-R_0/\sqrt{2})^2}}+\frac{1}{\sqrt{2}\sqrt{x^2+y^2+(z+R_0/\sqrt{2})^2}}\right],$$

$$\dot{v}=\left.\frac{\partial\varphi}{\partial s}\right|_{s=R_0}=-\frac{Q}{\sqrt{2}R_0^2}\left\{1-\left[3+2\sqrt{2}\cos\kappa\right]^{-3/2}\right\},$$

$$C=\sqrt{2}\pi\left[-1+2^{-1/2}\left(3-2\sqrt{2}\right)^{-1/2}\right],$$

$$\Omega_0^2\left(R_0,\frac{3\pi}{4}\right)=\Omega_0^{2*}(R_0)\frac{\left[-1+2^{-1/2}\left(3-2\sqrt{2}\right)^{-1/2}\right]}{2\left[1-\left(4-11\sqrt{2}/4\right)/4\right]}\approx 6.095\Omega_0^{2*}(R_0). \tag{18}$$

- $$\vartheta_c=\pi/6,\quad L=R_0,$$

$$\varphi=Q\left[\frac{1}{R_0}-\frac{1}{2(x^2+y^2+z^2)^{1/2}}-\frac{1}{\sqrt{x^2+y^2+(z-\sqrt{3}R_0/2)^2}}\right.$$

$$-\frac{1}{\sqrt{x^2+y^2+(z-\sqrt{3}R_0/2)^2}}+\frac{1}{\sqrt{3}\sqrt{x^2+y^2+(z-R_0/2\sqrt{3})^2}}$$

$$\left.+\frac{1}{\sqrt{3}\sqrt{x^2+y^2+(z+R_0/2\sqrt{3})^2}}\right],$$

$$\dot{v} = \left.\frac{\partial\varphi}{\partial s}\right|_{s=R_0} = \frac{Q}{R_0^2}\left\{1 - \frac{1}{\sqrt{2}\left[2-\sqrt{3}\cos\kappa\right]^{3/2}} + \frac{1}{\left[7-4\sqrt{3}\cos\kappa\right]^{3/2}}\right\},$$

$$C = 2\pi\left[1 + \sqrt{\frac{2}{3}}\left(2+\sqrt{3}\right)^{-1/2} - \frac{1}{2\sqrt{3}}\left(7+4\sqrt{3}\right)^{-1/2}\right],$$

$$\Omega_0^2\left(R_0, \frac{\pi}{6}\right) = \Omega_0^{2*}(R_0)\frac{(1/2)\left[1+\sqrt{\frac{2}{3}}\left(2+\sqrt{3}\right)^{-1/2} - \frac{1}{2\sqrt{3}}\left(7+4\sqrt{3}\right)^{-1/2}\right]}{\left[1-\left(2-\sqrt{3}/8\right)/4\right]} \approx 0.684\Omega_0^{2*}(R_0). \quad (19)$$

- $$\vartheta_c = 5\pi/6, \quad L = R_0,$$

$$\varphi = Q\left[\frac{1}{R_0} - \frac{1}{2(x^2+y^2+z^2)^{1/2}} - \frac{1}{\sqrt{x^2+y^2+(z-\sqrt{3}R_0/2)^2}} + \frac{1}{\sqrt{x^2+y^2+(z+\sqrt{3}R_0/2)^2}} - \frac{1}{\sqrt{3}\sqrt{x^2+y^2+(z-R_0/2\sqrt{3})^2}} + \frac{1}{\sqrt{3}\sqrt{x^2+y^2+(z+R_0/2\sqrt{3})^2}}\right],$$

$$\dot{v} = \left.\frac{\partial\varphi}{\partial s}\right|_{s=R_0} = \frac{Q}{R_0^2}\left\{1 - \frac{1}{\sqrt{2}\left[2+\sqrt{3}\cos\kappa\right]^{3/2}} + \frac{1}{\left[7+4\sqrt{3}\cos\kappa\right]^{3/2}}\right\},$$

$$C = 2\pi\left[1 - \sqrt{\frac{2}{3}}\left(2-\sqrt{3}\right)^{-1/2} + \frac{1}{2\sqrt{3}}\left(7-4\sqrt{3}\right)^{-1/2}\right],$$

$$\Omega_0^2\left(R_0, \frac{5\pi}{6}\right) = \Omega_0^{2*}(R_0)\frac{(1/2)\left[1-\sqrt{\frac{2}{3}}\left(2-\sqrt{3}\right)^{-1/2} + \frac{1}{2\sqrt{3}}\left(7-4\sqrt{3}\right)^{-1/2}\right]}{\left[1-\left(2-\sqrt{3}/8\right)/4\right]} \approx 18.657\Omega_0^{2*}(R_0). \quad (20)$$

The limiting case $\vartheta_c \to 0$ when the bubble wall is tangent to rigid boundary in one point has been analysed earlier [11] where it was shown that the fundamental frequency there is

$$\Omega_0^2(R_0, 0) = \ln 2\Omega_0^{*2}(R_0). \quad (21)$$

Although we presented results for the contact angles equal even fraction of π, the similarly expressions can be obtained and for odd fractions ones, but the corresponding formulae for the potential and especially for the normal displacements at bubble wall have cumbersome form (see

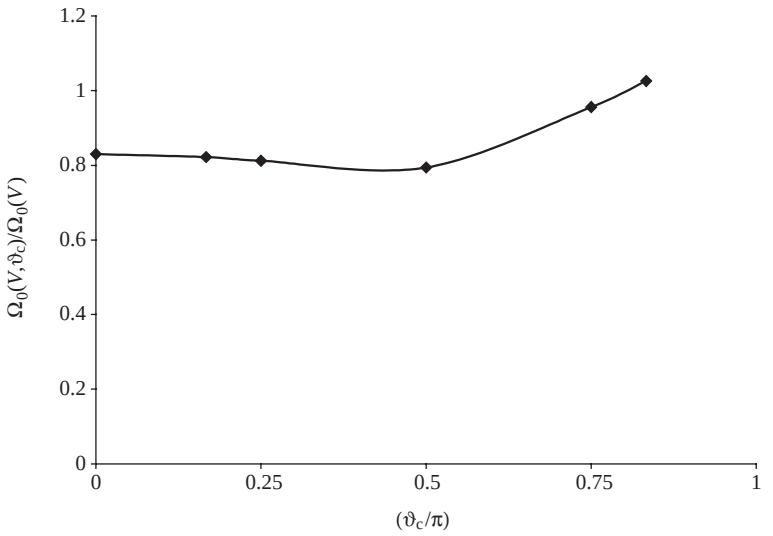

Fig. 3. Dependence of the natural frequency of the tethered bubble with fixed volume $\Omega_0(V,\vartheta_c)$ on the contact angle ϑ_c. The normalisation on the natural frequency $\Omega_0^*(V)$ of the free bubble with the same volume is used.

Appendix A for $\vartheta_c = \pi/3$) and thus have a little preferences in comparison with integral representation.

The derived expressions for the natural frequencies (17)–(21) are given for the fixed radius of curvature R_0 of spherical segment, but it is more interesting to trace how does the natural frequency of the bubble with the fixed volume $V = (4\pi/3)R_0^3$ vary as it is tethered to the wall and the contact angle is changed?

$$\Omega_0^2(V,\vartheta_c) = \Omega_0^{*2}(V)\frac{\sin\vartheta_c C(\vartheta_c)}{2\left[1-\dfrac{(1-\cos\vartheta_c)^2(2+\cos\vartheta_c)}{4}\right]^{1/3}}. \tag{22}$$

Fig. 3 illustrates the dependence of $\Omega_0(V,\vartheta_c)/\Omega_0^*(V)$ on the contact angle ϑ_c, here $\Omega_0^*(V)$ is the natural frequency of the free bubble. This nonmonotonic relation is surprising at first glance, but can be explained the following way. As the oscillating gas bubble is approached to the rigid boundary its inertial mass is increased. Really as has been mentioned above the presence of rigid boundary is equivalent to the presence of the mirror bubble oscillating synchronous with the first one. Now it is more difficult for the bubble to accelerate the fluid in the region between its mirror, as the second (mirror) bubble acts with opposite force. As a result the inertial mass grows and the fundamental frequency decreases as the bubble is approached to the boundary. When the bubble touch the boundary ($\vartheta_c = 0$), the area where the bubble and its mirror hinder each other to accelerate the fluid begin to shrink and as a result the inertial mass will decrease, the natural frequency begin to increase. This growth will continue till the limit of applicability our approach — homobaricity within the bubble that is till the wavelength will be compared with base of the spherical segment $L = 2R_0\sin\vartheta_c = 2(3V/4\pi)^{1/3}\sin\vartheta_c\left[1-(1-\cos\vartheta_c)^2(2+\cos\vartheta_c)/4\right]^{-1/3}$.

It would be of interest to compare present findings with the 'opposite' case of the bubble oscillating in the vicinity of a nearly plane free surface. This problem is however more complicated due to the possible distortion of the free surface. Two limiting case has been analysed by Prosperetti and his colleagues [15,16]. The dimensionless frequency of the volume mode of a small bubble floating at the surface of a liquid before bursting depends on the single dimensionless parameters (L_0/D) (here L_0 is the radius of a spherical bubble that would contain the same amount of gas as the floating bubble at the same internal pressure, D is the so-called capillary length) and this dependence is not monotonic [15]. The linear oscillation frequency of a bubble in the vicinity of a distorted plane free surface has been calculated by a perturbation method in Ref. [16]. The solution of the problem is greatly facilitated by the use of approach initially derived by Strasberg [17]. The natural frequency diverges logarithmically as the bubble approaches the plane free surface. However, the deviation from 1 is significant only for depths of immersion of the bubble smaller than about three bubble radii [16].

In conclusion one should point out that although the primary aim of this work was to analyse volume oscillations of tethered bubbles in laboratory studies, the final results are equally applied (with substitution of the compressibility of the gas in a single bubble by the compressibility of bubble–liquid mixture) for the evaluation of fundamental frequencies of collective oscillations of gas plumes — seepage of hydrocarbon deposits at ocean bottom [18,19].

Acknowledgements

This work has been supported by The Russian Fund for Basic Research under grants numbers 01-05-64915 and 04-02-16412.

Appendix A

Potential for the contact angle $\vartheta_c = \pi/3$.

$$L = \sqrt{3}R_0$$

$$\bullet \quad \varphi = \frac{Q}{\pi}\left\{\frac{[-\arccos(A) + \arccos(-A)]}{\sqrt{3}R_0} + \frac{1}{\sqrt{3}}\frac{[\arccos(B) - \arccos(-B)]}{\sqrt{x^2 + y^2 + (z - R_0/2)^2}} + \frac{1}{\sqrt{3}}\frac{[\arccos(D) - \arccos(-D)]}{\sqrt{x^2 + y^2 + (z + R_0/2)^2}}\right\},$$

$$A = \sqrt{\frac{\sqrt{\left(\tilde{r}^2 - 3R_0^2/4\right)^2 + 3z^2R_0^2} + \left(\tilde{r}^2 - 3R_0^2/4\right)}{\sqrt{\left(\tilde{r}^2 - 3R_0^2/4\right)^2 + 3z^2R_0^2} + \left(\tilde{r}^2 + 3R_0^2/4\right)}}, \ (\tilde{r}^2 \equiv x^2 + y^2 + z^2),$$

$$B = \sqrt{\frac{\sqrt{\left(\tilde{r}^2 - 3R_0^2/4\right)^2 + 3z^2R_0^2} - (1/2)\left(\tilde{r}^2 - 3R_0^2/4\right) + (3/2)zR_0}{\sqrt{\left(\tilde{r}^2 - 3R_0^2/4\right)^2 + 3z^2R_0^2} + \left(\tilde{r}^2 + 3R_0^2/4\right)}},$$

$$D = \sqrt{\frac{\sqrt{\left(\tilde{r}^2 - 3R_0^2/4\right)^2 + 3z^2R_0^2} - (1/2)\left(\tilde{r}^2 - 3R_0^2/4\right) - (3/2)zR_0}{\sqrt{\left(\tilde{r}^2 - 3R_0^2/4\right)^2 + 3z^2R_0^2} + \left(\tilde{r}^2 + 3R_0^2/4\right)}}.$$

References

[1] T.G. Leighton, A.D. Phelps, D.G. Ramble, D.A. Sharpe, Comparison of the abilities of eight acoustic techniques to detect and size a single bubble, *Ultrasonics* 34 (1996) 661–667.

[2] P.R. Birkin, Y.E. Watson, T.G. Leighton, K.L. Smith, Electrochemical detection of Faraday waves on the surface of a gas bubble, *Langmuir Surfaces and Colloids* 18 (2002) 2135–2140.

[3] A.J. Hardwick, The mechanism of subharmonic ultrasound modulation by forcibli oscillating bubbles, *Ultrasonics* 33 (1996) 341–343.

[4] J.B. Blake, B.B. Taib, G. Doherty, Transient cavities near boundaries—part 1: rigid boundary, *Journal of Fluid Mechanics* 170 (1986) 479–497.

[5] J.B. Blake, D.C. Gibson, Cavitation bubbles near boundaries, *Review to Fluid Mechanics A* 19 (1987) 99–123.

[6] K. Sato, Y. Tomita, A. Shima, Numrical analysis of a gas bubble near a rigid boundary in an oscillating pressure field, *Journal of the Acoustical Society of America* 95 (1994) 2416–2424.

[7] J.R. Blake, G.S. Keen, R.P. Tong, M. Wilson, Acoustic cavitation: the fluid dynamics of non-spherical bubbles, *Philosophical Transactions of the Royal Society of London A* 357 (1999) 251–267.

[8] A. Prosperetti, Bubble phenomena in sound field—part 2, *Ulttrasonics* 22 (1984) 115–124.

[9] M. Longuet-Higgins, Monopole emission of sound by asymmetric bubble oscillations—part 1: normal modes, *Journal of Fluid Mechanics* 201 (1989) 525–541.

[10] R.H. Cole, *Underwater Explosions*, Princeton University Press, Princeton, 1948.

[11] Yu.A. Kobelev, L.A. Ostrovskii, Acousto-electrostatic analogy and gas bubbles interaction in liquid, *Soviet Physics Acoustics* 30 (1984) 715–716.

[12] W.R. Smythe, *Static and Dynamic Electricity*, McGraw-Hill, New York, 1950.

[13] L.D. Landau, E.M. Lifshitz, *Electrodynamics of Continuos Medium*, Nauka, Moscow, 1982 (in Russian).

[14] H.M. Macdonald, *Electromagnetism*, Bell, London, 1934.

[15] N.Q. Lu, The oscillations of a small floating bubble, *Physics of Fluids A* 1 (1989) 252–260.

[16] H.N. Oguz, A. Prosperetti, Bubble oscillations in the vicinity of a nearly plane surface, *Journal of the Acoustical Society of Amercia* 87 (1990) 2085–2092.

[17] M. Strasberg, The pulsation frequency of nonspherical gas bubbles in liquids, *Journal of the Acoustical Society of America* 25 (1953) 536–537.

[18] I. Leifer, R.K. Patro, The bubble mechanism for methane transport from the shallow sea bed to the surface: a review and sensitivity study, *Continental Shelf Research* 22 (2002) 2409–2428.

[19] A.O. Maksimov, Acoustics of marine hydrocarbon seeps, *Proceedings of Fifth World Congress on Ultrasonics*, Paris, September 2003, pp. 229–232.